Volume 21, No 4 | International Journal of Radiation Research, October 2023

Neuroprotective effect of polyethylene Glycol (PEG-3350) on radiation-induced brain injury via membrane stabilization

I.H. Sever[1], B. Ozkul[2], O. Atasoy[3], N. Cini[3], M.F. Bozkurt[4], M.A. Erdogan[5*], G. Yaprak[3], O. Erbas[6]

[1]Demiroglu Bilim University, School of Medicine, Department of Radiology, Istanbul, Turkey
[2]Istanbul Atlas University, School of Medicine, Department of Radiology, Istanbul, Turkey
[3]Kartal Dr. Lutfi Kirdar Training and Research Hospital, Department of Radiation Oncology, Istanbul, Turkey
[4]Afyon Kocatepe University, Faculty of Veterinary Medicine, Department of Pathology, Afyonkarahisar, Turkey
[5]Izmir Katip Celebi University, Department of Physiology, Izmir, Turkey
[6]Demiroğlu Bilim University, School of Medicine, Department of Physiology, Istanbul, Turkey

► *Original article*

***Corresponding author:**
Mumin A. Erdogan, DVM, Ph.D.,
***E-mail:** alpero86@gmail.com*

Received: March 2023
Final revised: May 2023
Accepted: June 2023

Int. J. Radiat. Res., October 2023; 21(4): 733-743

DOI: 10.52547/ijrr.21.4.19

Keywords: *Radiation, PEG-3350, MRS, 8-oxo-dG, BDNF, membrane stabilization.*

ABSTRACT

***Background*:** This research aims to evaluate whether polyethylene glycol (PEG), which can immediately repair neuronal membranes, will have a protective effect against radiation-induced brain injury (RIBI). ***Materials and Methods*:** Whole brain irradiation (RAD) procedure was performed on 14 of 21 rats included in the study for establishing RIBI. Rats were randomly divided into three groups containing equal numbers of animals: control (RAD not established), placebo (RAD applied, and treated with 1 ml/kg/day of saline that was administered intraperitoneally), and treatment (RAD applied, and treated with 30 mg/kg /day of PEG 3350 that was administered intraperitoneally). Following the end of the 22-day treatments, behavioral tests were performed first, and then magnetic resonance spectroscopy (MRS) was applied to measure brain lactate levels. All rats were sacrificed in order to perform biochemical analysis and histopathological examination of brain tissue. ***Results*:** Compared to the control group, MDA, TNF-α, NF-κB and lactate levels were significantly increased, while BDNF levels were decreased in the placebo group; and RAD-induced changes in all these biochemical markers were reversed by PEG. In MRS performed from the corpus striatum, there was an evident decrease in lactate levels after PEG treatment. Impairment in memory and learning was more limited in PEG-treated rats than in the rats receiving saline therapy. Furthermore, histological examinations from hippocampus and cerebellum exhibited that PEG treatment significantly reduces apoptosis, astrogliosis, and oxidative DNA damage in rats. ***Conclusion*:** Our results support that PEG is very effective in preventing RIBI with its secondary effects on the basis of membrane stabilization.

INTRODUCTION

For both primary and metastatic brain cancers, radiation therapy is an increasingly popular and successful treatment that offers long-term survival in many patients [1]. The success of treatment and the rate of tumor control both rise with higher radiation doses. However, in this situation, the danger of negative effects on healthy brain tissue also rises, which leads to substantial neurological issues, particularly cognitive loss, which greatly lowers the quality of life [2, 3]. Finding a successful treatment for radiation-induced brain injury (RIBI) is crucial in order to preserve the patient's quality of life in addition to concentrating on overall survival because 50% of patients may experience irradiation-induced injury to nearby brain tissues after treatment [4, 5].

RIBI is divided into three stages: acute, early delayed, and late delayed [6] based on the progression of the clinical symptoms and the amount of time after the first event. While acute and early delayed harms are often momentary and reversible, late delayed impacts are frequently permanent. It is known that epigenetic alterations, apoptosis, poor cell proliferation and differentiation, oxidative stress, and neuroinflammation are some of the significant underlying components [7–13], even if the mechanisms that may induce radiation damage are not entirely understood. By directly ionizing DNA or by indirectly producing free oxygen radicals, radiation may damage DNA [14]. Additionally, radiation creates reactive oxygen species (ROS) by ionizing the water in the surrounding environment. ROS are responsible for lipid peroxidation by oxidizing macromolecules [7-9]. As a result, products of protein and lipid oxidation increase.

[Downloaded from ijrr.com on 2026-11-09]

[DOI: 10.61186/ijrr.21.4.733]

In spite of the fact that mitochondria constitute a significant generator of reactive oxygen species (ROS) in cells, they are also a frequent site of oxidative damage [15, 16]. Proteins in the respiratory complex, lipid peroxidation, and DNA damage are all brought on by oxidative stress in mitochondria. Radiation has been found to cause mitochondrial-induced cellular damage, particularly in the central nervous system, in addition to its effects on oxidative stress and neuroinflammation [17–19]. This damage is caused by the significant degradation of a number of mitochondria-specific proteins. Lactic acidosis owing to reduced adenosine triphosphate synthesis is the most often documented laboratory anomaly in individuals with mitochondrial diseases [20]. In addition, one of the areas damaged by radiation in the brain is the basal ganglia [21] and basal ganglia disease etiology is heavily influenced by mitochondrial dysfunction [22-24]. Therefore, measuring lactate concentrations from basal ganglia, an anaerobic by-product of glycolysis, can provide information about radiation-induced mitochondrial damage. The non-invasive, radiation-free magnetic resonance spectroscopy (MRS) method is used in conjunction with magnetic resonance imaging (MRI) to measure the levels of metabolites in tissues. The measurement of lactate in small-sized animal brains can be performed non-invasively with high accuracy with the MRS examination performed with a device with a magnetic field strength of 3T [25-27].

Radiation greatly increases neuroinflammation in brain tissue, particularly in the hippocampus, according to a number of preclinical investigations [10 -12]. Radiation in this circumstance activates genes associated with inflammation and overexpresses pro-inflammatory proteins, as is particularly evident in acute-phase RIBI. After the NF-κB pathway is activated, a transcription factor essential to the inflammatory process, pro-inflammatory substances like interferon-gamma (INF-γ), tumor necrosis factor-alpha (TNF-α), and interleukin-1 beta (IL-1β) increase quickly (within hours) [28-30]. These cytokines, particularly TNF-α, are linked to hypoxia, which causes reactive astrogliosis brought on by radiation as well as vascular damage that compromises the blood-brain barrier [31].

About %60 of juvenile brain cancers are posterior fossa tumors, and irradiation is one of the most successful therapies. The experiments undertaken demonstrate that the breakdown of the blood-brain barrier after irradiation varies across brain areas, with the cerebellum being the most vulnerable region in this regard [32, 33]. In particular, it has been proven that Purkinje cells located in the germinal zone of the cerebellum show a number and morphological deterioration even with low-dose radiation exposure, such as 0.5 Gy, during the gestational period [34]. Because it includes areas where neurogenesis continues, the hippocampus, a crucial area of the brain involved in the development, organization, and storage of memory, is also one of the most radiation-sensitive brain regions [35, 36]. Studies have shown that the death of certain highly proliferative hippocampal cells after radiation treatment may be the primary factor contributing to cognitive impairment [36, 37]. Therefore, studies specific to these regions, including behavioral tests, may provide useful information in evaluating radiation-related brain damage and possible treatment options.

Regardless of the method of administration, the water-soluble polymer polyethylene glycol (PEG) has extremely low immunogenic and toxic characteristics and has been approved for use in food, cosmetics, and medicines [38, 39]. For kidney, pancreatic, and liver transplants, PEGs are clinically added to organ preservation solutions to lessen the harm done by cold ischemia-reperfusion [40]. PEGs have been shown to reduce oxidative stress by stabilizing cell membranes in a number of experimental investigations that have recently been reported [41, 42]. Again, based on PEG's protective impact on cell membrane permeability, studies are finding that it indirectly reduces inflammation by lowering NF-κB and TNF-α levels [43, 44]. Additionally, Chen et al. found in another investigation that PEG physically covers diseased holes in the mitochondrial membrane and enhances general neurological performance by avoiding direct mitochondrial damage [45]. PEGs may be a suitable alternative to prevent and treat RIBI given the currently known advantages of the drugs.

The goal of this research was to investigate the protective impact of PEG in RIBI by measuring the levels of NF-κB, TNF-α, lactate, malondialdehyde (MDA), and brain-derived neurotrophic factor (BDNF) and comparing these markers with histology and MRS data. This is the first study to examine the therapeutic and protective roles of PEG in RIBI with MRS findings, behavioral analysis, histological findings, and biochemical outcomes.

This study offers an innovative exploration into the potential protective effects of Polyethylene glycol (PEG) against radiation-induced brain injury (RIBI). It leverages a multi-dimensional approach, employing Magnetic Resonance Spectroscopy (MRS) to non-invasively investigate radiation-induced mitochondrial damage, coupled with histological examinations and biochemical assays to assess various indicators of oxidative stress, neuroinflammation, and neuronal function. This research marks the first instance where the therapeutic role of PEG in RIBI is scrutinized via MRS findings, behavioral analysis, histological studies, and biochemical outcomes together, creating a comprehensive analysis that gives a more holistic view of the potential benefits of PEG. This approach may shed light on new therapeutic strategies for protecting brain function during radiation therapy, thus improving patient quality of life and overall

[Downloaded from ijrr.com on 2026-11-09]

[DOI: 10.61186/ijrr.21.4.733]

survival rates.

MATERIALS AND METHODS

Animals

Each male Wistar albino rat weighed 250-300 grams and was 10-11 weeks old when included in this experiment. The Wistar albino rats used in this experiment were provided by the Laboratory Animal Research Center of Demiroglu Science University. The rats had access to food and water in a temperature-controlled (22 ± 2 °C), photoperiodic (12-hour light/dark) environment. Our study methods and procedures were guided by the National Institutes of Health's Guidelines for the Care and Use of Laboratory Animals (USA) [46]. Study protocol has been approved by the he Animal Ethics Committee of Demiroglu Science University (Ethics Number: 4211121). The experiment was carried out using rats given by our university's laboratory.

Experimental procedures

To create a model of RIBI, rats were randomly divided into 3 groups, and a total of 14 rats in the group containing two equal numbers of rats underwent whole brain irradiation (RAD). No therapy or irradiation was administered to the seven remaining rats, who were designated as the control group. The set-up of the working groups was as follows: Group 1: Non-irradiated (control) (no irradiation or treatment applied, n=7); Group 2: Saline-treated (placebo) (RAD + 1 mL/kg/day intraperitoneal injection of 0.9% NaCl, n=7); Group 3: PEG treatment [RAD + 30 mg/kg/day intraperitoneal injection of PEG 3350 (Merck), n=7]. All treatments were applied for a total of 22 days, starting 7 days before RAD and ending 15 days after. Following the treatment period, behavioral tests was conducted on the 23rd and 24th days, between 10:00 and 15:00. At the end of behavioral testing, MRS imaging was performed on all rats under ketamine (50 mg/kg)/ xylazine (10 mg/kg) anesthesia. For biochemical and histological analysis, brains of all animals were removed after anesthetization with ketamine (100 mg/kg) and xylazine (50 mg/kg) at the end of the research. Figure 1 depicts the research process in broad strokes.

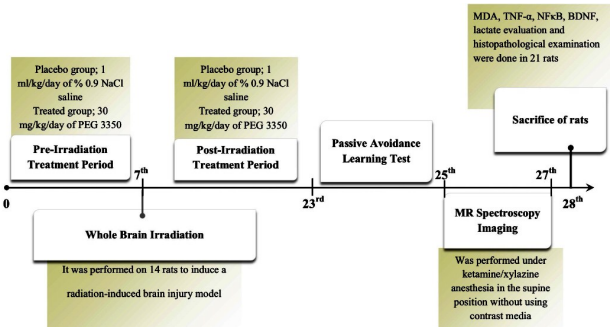


Figure 1. Timeline showing the study protocol.

Irradiation Procedure

The Eclipse treatment planning system (TPS) from Varian Medical Systems, Palo Alto, California, USA, was used to run a rat simulation using a 1 mm cross-sectional computed tomography scan (CT simulator GE Bright Speed). There was a dosage calculation carried out using Anisotropic Analytical Algorithm (AAA system version 13.7.20). The administration dose of 30 Gy was selected because it corresponds to a BED (Biologically effective dose) of 153 Gy (α/β = 3 Gy) [47]. On CT images, the rat brain tissue was identified by the radiation oncologist, and planning was carried out so that the entire brain tissue received 98% of the prescribed dose. 100 cm for the source skin distance (SSD) and 6MV for the irradiation energy were chosen, and irradiation was planned on the Varian DHX Linear Accelerator (Linac). Finally, the skin dose at the beam entrance was taken into account before the irradiation plan was approved.

Rats were placed in the prone position after being given a combination of 50 mg/kg ketamine and 10 mg/kg xylasine for anesthesia before having their skulls irradiated with a single dose of 30 Gy at a dosage rate of 1 Gy/min. Irradiation was carried out in tubes made of Plexiglas (1.18g/cm^3) that were intended to effectively confine sedated animals underneath the irradiation region and reduce uncertainty in animal tests (figure 2). The animals were put back in their cages after the radiation treatment.

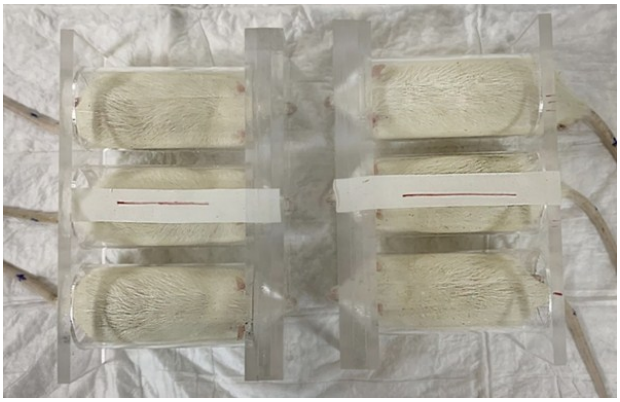


Figure 2. The image of rats that will be subjected to whole brain irradiation in plexiglass tubes designed for immobilization. Rats anesthetized in the prone position underwent skull irradiation with a single dose of 30 Gy at a dose rate of 1 Gy/min.

Passive avoidance learning (PAL) test

Rat's capacity to learn and remember were assessed using a test that elicited fear in the test subjects. The PAL box is designed to contain light and dark rooms with dimensions of 20×40×20 cm. A guillotine door, which shut when a rat entered, divided the two halves. The door that separates the dark and light rooms opened after about ten seconds of adaptation. Because they believe the dark compartment is more secure, rats tend to avoid light

[Downloaded from ijrr.com on 2026-11-09]

[DOI: 10.61186/ijrr.21.4.733]

in normal situations. The guillotine door was closed and the rats were given a 1.5 mA electric shock lasting three seconds as soon as they were fully enclosed in the dark chamber. The rat was carried back to its cage and placed inside after having some time to explore the pitch blackness. The rats were returned to their original containers the next day, and no electric shocks were administered since it was possible to see how long it took a rat to go from a bright room to a dark room. There was a maximum delay of 300 seconds. This period of time was taken into consideration as a measure of how long it took the rats to realize they should not join the evil side.

MRI and MR spectroscopy

Without contrast medium, a 3.0 T clinical magnetic resonance imaging/MRS scanner (GE SIGNA ™ Pioneer, Piscataway, New Jersey) was used for all examinations. Intraperitoneal injections of ketamine and xylazine were used to anesthetize the rats in this study. Motion artifacts were minimized with the use of a plastic head holder designed specifically for the scanning table. In order to keep the rats' body temperatures stable during the imaging session, a water heating pad was used. Excitation and detection of signals were performed with a 16-channel flexible coil (GE Healthcare, Piscataway, NJ, USA). Following the acquisition of localizers, 12 slices of T2 weighted spin-echo images, with a TR/TE of 2690 ms, a FOV of 33×33 mm^2, section thickness of 2 mm, 256×256 pixels, 175Hz/ pixel bandwidth and two acquisitions, were obtained and the examination was terminated by spectroscopy. The right corpus striatum was chosen as the area to be examined by spectroscopy. An array of 24/24 x/y phase coding, 1000 ms repeat time, 35 ms echo time, 2×2×4 mm voxel dimensions, and an excitation number of 1 was employed for 1H-MRS analysis. The amounts of lactate in the striatum of rats in all groups were evaluated by comparing the spectra (1.3 ppm for lactate) obtained from a 16 µl volume of each rat. Free induction decay signal measurement yielded MRS by Fourier transformation. GE Healthcare software was used to process data from a workstation. MRS' findings were examined by a radiologist with ten years of expertise in neuroimaging who was not aware of the focus group data.

Hippocampus and cerebellum histopathology

It was chosen to examine the hippocampus and cerebellum for any symptoms of radiation damage in the Cornu Ammonis (CA) 1 and 3 areas. Rat brains were extracted and preserved for five days in 10% formaldehyde in 0.1 M phosphate-buffered solution after MRS imaging. The brains were coronally sectioned on a spinning microtome at 6 m and put on adhesive-coated slides. In order to reduce endogenous peroxidase activity before blocking with serum blocking solution for 15 minutes at room temperature, brain slices were treated with H2O2 (3%) for 20 minutes. Sections were then treated with primary antibodies for GFAP (RB-087, Thermo Scientific, 1/50 dilution) and 8-Oxo-2'-deoxyguanosine (8-Oxo-dG) (sc-66036, Santa Cruz Biotechnology, 1/200 dilution) for 24 hours at 4 °C. 3-amino-9-ethyl carbazole (AEC, TA-125-HA Thermo Scientific) was used to see the finished result after the ABC kit (Vectastain Elite ABC HRP Kit PK-6101, Vector Laboratories) was utilized to identify antibodies. The Axiocam ICc 5 digital camera was installed on a Zeiss Lab A1 microscope to take photos of all the slides. Images were then processed using the ZEN2 image analysis system and image J.

Positive cells were counted at a magnification of 40x in three to four random sections for each rat to determine the GFAP and 8-Oxo-dG immune staining indices. In four stages for each group being researched, these operations are carried out using an image analysis system (Image-Pro Express 1.4.5, Media Cybernetics, Inc. USA).

In formalin-fixed tissue, the Nissl substance in the cytoplasm of neurons is stained using a Cresyl Violet Acetate solution. Neuropil is distinguished by this dye as granular purple-blue staining. Using the same image analysis equipment, six slices of Cresyl violet staining from each group were examined for the number of neurons that survived. The same researcher, who was blind to the focus groups, did all the histopathology investigations.

Brain biochemical analysis

The rats were promptly decapitated, and the brains were collected and stored at -20°C for biochemical analysis. After homogenizing the brain tissues in five liters of phosphate-buffered saline (pH 7.4), they were centrifuged at 5000 rpm for 15 minutes. Using ELISA kits (Biosciences, Abcam) that are readily accessible in the marketplace, we determined the concentrations of TNF-α, NF-κB, BDNF, and lactate in brain supernatants. Each animal sample's results were replicated in accordance with the producer's instructions. The absorbance was measured using a micro plate reader (ELX808, BioTek, Santa Clara, CA, USA).

The protein quantity in samples of brain tissue was assessed using the Bradford test, a spectroscopic analytical technique [48]. As a reference protein or protein standard, bovine serum albumin was selected since it is a conveniently accessible protein with characteristics comparable to the protein whose level must be approximated.

To identify lipid oxidation, MDA levels were assessed using the thiobarbituric acid reactive substance (TBARS) test. The brain tissue samples were employed using the TBARS reagent and trichloroacetic acid at a temperature of 100 degrees Celsius. After centrifuging the samples at 3000 rpm for 20 minutes, the supernatant was removed, and the absorbance at 535 nm was calculated. A standard

[Downloaded from ijrr.com on 2026-11-09]

[DOI: 10.61186/ijrr.21.4.733]

calibration curve was used to calculate the MDA concentrations, which were then represented in nanomoles per gram of protein.

Statistical analysis

The data was analyzed using the Windows version of SPSS 15.0. (SPSS Inc. Chicago, IL, USA). The standard deviation is subtracted from the mean (SEM). When evaluating the variance for homogeneity and normality, the Levene's and Shapiro-Wilk tests were used. All variables had to pass the normality test in order to be considered normal. Using an ANOVA with Bonferroni correction, the parametric variables were evaluated. To be considered statistically significant, p-values of 0.05 or less were required.

RESULTS

A total of 33 rats were used, of which 21 were included in the study. Of the 7 rats included in the placebo group, 4 (2 on the same day, and the others on the third and sixth days, respectively) died due to irradiation. With the death of 6 of the 10 rats (3 on the same day, and the others on the 4th, 5th and 8th days, respectively) added later, the number of placebo group was completed to 7. Similarly, 2 rats (same day as irradiation and on the third day) in the PEG-treated group died secondary to irradiation, and new rats were added. The study was continued by adding another rat on the same day to replace each deceased rat. Although the study template was calculated as 28 days, the study took approximately 40 days in total.

Biochemical parameters

All results of biochemical parameters are presented in table 1. Rats in the radiation-induced brain injury model were found to have significantly greater ($p<0.001$) levels of MDA in the placebo group (89.3±10.6 nmol/gr protein) than they did in the control group (45.3±5.1 nmol/gr protein). The antioxidant action of PEG, on the other hand, resulted in considerably lower ($p<0.05$) MDA levels in PEG-treated rats (57.4±8.5 nmol/gr protein) than saline-treated rats.

Again, in parallel with MDA, the levels of NF-κB and TNF-α in the saline-treated rats (130.1±14.3 pg/mg protein and 139.3±16.7 pg/mg protein, respectively) were significantly increased ($p<0.001$ both) compared to non-irradiated rats (9.7±1.17 pg/mg protein and 16.6±2.8 pg/mg protein, respectively). Due to the indirect anti-inflammatory effect of PEG, these biochemical markers of radiation-induced inflammation were significantly lower ($p<0.05$ and $p<0.01$, respectively) in the group receiving therapy (73.5±11.5 and 71.5±6.8 pg/mg protein, respectively) than in the placebo group.

Lactate levels were assessed in brain homogenates in order to investigate the effects of radiation on mitochondrial functioning. Rats in the placebo group had greater ($p<0.001$) lactate levels (2.21±0.3 mmol in 100 g) than rats in the control group (1.16±0.13 mmol in 100 g). Lactate levels in the PEG-treated rats (1.2±0.25 mmol in 100 g) were much lower ($p<0.05$) than in the saline-treated rats as a result of PEG's influence on membrane stability.

Additionally, we looked at how radiation and PEG affected neurogenesis using BDNF, a crucial neurotrophic factor for neuron proliferation and differentiation. Saline-treated rats had considerably lower levels of BDNF (0.9±0.1 pg/mg protein) than non-irradiated rats (2.3±0.2 pg/mg protein; $p<0.001$). However, brain BDNF levels from the treated rat group (2.07±0.3 pg/mg protein) were shown to be statistically substantially higher ($p<0.05$) than those from the control group, demonstrating the beneficial effects of PEG on neurogenesis.

Table 1. Comparative Analysis of the Impact of Radiation Treatment and PEG on Biochemical Parameters in the Brain.

	Normal Control	Brain Irradiation + Saline	Brain Irradiation + PEG
Brain MDA level (nmol/gr protein)	45.3 ± 5.1	89.3 ± 10.6 **	57.4 ± 8.5 #
Brain TNF-α level (pg/mg protein)	16.6 ± 2.8	139.3 ± 16.7 **	71.5 ± 6.8 ##
Brain NF-κB level (pg/mg protein)	9.7 ± 1.17	130.1 ± 14.3 **	73.5 ± 11.5 #
Brain Lactate level (mmol/100 g wet weight)	1.16 ± 0.13	2.21 ± 0.3 **	1.2 ± 0.25 #
Brain BDNF level (pg/mg protein)	2.3 ± 0.2	0.9 ± 0.1 **	2.07 ± 0.3 #

Histopathological findings

All histopathological findings are presented in table 2 cresyl violet staining was used to determine the count and the morphology of surviving neurons both in the cortex of the cerebellum (figure 3) and CA1-CA3 regions of the hippocampus (figure 4). Concerning the damage caused by irradiation to neurons, the number of pyramidal neurons reduced dramatically ($p<0.001$ for CA1 and $p<0.01$ for CA3) in the saline-treated rats (52.6±3.08 and 29.4±1.5, respectively) than in the non-irradiated rats (80.2±3.1 and 45.8±2.3, respectively). These results suggest that hippocampal neurons experience apoptosis as a cause of radiation-induced brain damage. In addition, the number of pyramidal neurons in the PEG-treated rats (69.4±3.3 and 37.6±1.7, respectively) was substantially closer ($p<0.001$ for CA1 and $p<0.05$ for CA3) to that of the non-irradiated rats than in the placebo group rats (figure 4). However, when we observed the diameters and counts of Purkinje cells in the cerebellum; although we found a certain decrease due to irradiation (13.3±1.2 μm and 20.8±0.9,

[Downloaded from ijrr.com on 2026-11-09]

[DOI: 10.61186/ijrr.21.4.733]

respectively) and a slight increase with PEG treatment (14.07±0.6 µm and 21.5±1.2, respectively), the findings were not statistically significant (table 2).

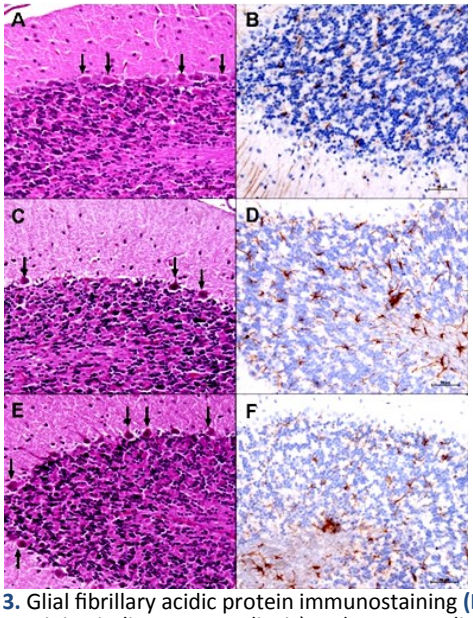


Figure 3. Glial fibrillary acidic protein immunostaining **(B, D, F)** (brown staining indicates astrogliosis) and Hematoxylin-eosin staining **(A, C, E)** of the cerebellar cortex with x40 magnification. A-B: Histological image of the cerebellum of a rat in the control group shows normal gliotic activity and Purkinje neurons (arrows). **C-D:** Dysmorphological changes in Purkinje neurons and an increase in glial activity were observed in the cerebellum of the rat that received whole brain irradiation (RAD) and saline treatment. **E-F:** In the rat treated with PEG 3350, the increase in glial activity and dysmorphic changes in Purkinje neurons were observed to be more limited compared to the placebo group. (Scale bar= 50 µm).

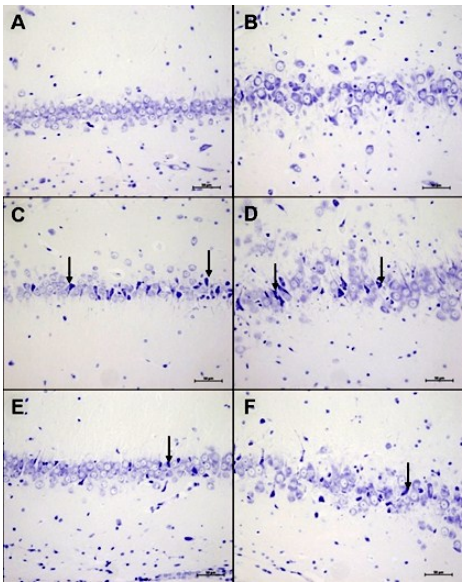


Figure 4. Cresyl violet-stained images of Cornu Ammonis 1 (CA1) **(A, C, E)** and CA3 regions **(B, D, F)** of the hippocampus with x40 magnification. **A-B:** Pyramidal neurons with normal count and morphology are observed in CA1 and CA3 regions of the rat in the control group. **C-D:** Histological sections of the CA1 and CA3 regions of an irradiated and saline-treated rat show degenerations of the neuronal body and decrease in the count of pyramidal neurons. **E-F:** In a rat treated with PEG 3350, dysmorphic and numerical changes in pyramidal neurons were observed to be more limited compared to the placebo group. (Scale bar= 50 µm).

Table 2. Comparative analysis of the effects of radiation treatment and PEG on brain histopathological findings.

	Normal Control	Brain Irradiation + Saline	Brain Irradiation + PEG
Neuronal Count CA1	80.2 ± 3.1	52.6 ± 3.08 **	69.4 ± 3.3 ##
Neuronal Count CA3	45.8 ± 2.3	29.4 ± 1.5*	37.6 ± 1.7 #
GFAP immunostaining index (CA1)	23.6 ± 1.2	39.3 ± 1. 7 *	28.8 ± 1.9 #
GFAP immunostaining index (CA3)	21.3 ± 1.1	37.2 ± 1.6 *	25.1 ± 0.8 #
8-Oxo-2'- deoxyguanosine immunostaining index (CA1)	1.1 ± 0.07	12.8 ± 0.5 **	4.01 ± 0.2 ##
8-Oxo-2'-deoxyguanosine immunostaining index (CA3)	0.8 ± 0.01	13.7 ± 0.4 **	3.9 ± 0.7 ##
Purkinje Count Cerebellum	23.5 ± 1.5	20.8 ± 0.9	21.5 ± 1.2
Purkinje Diameter Cerebellum (µm)	18.9 ± 0.5	13.3 ± 1.2	14.07 ± 0.6
GFAP immunostaining index (Cerebellum)	20.9 ± 1.5	41.4 ± 1.1 *	27.9 ± 0.8 #

According to studies, radiation-induced astrogliosis may be brought on by the molecules that irradiated microglial cells release [13, 31]. As a result, we used GFAP staining to show gliosis in the CA1-CA3 regions of the hippocampus (figure 5) and the cerebellar cortex (figure 3). In comparison to the control group (23.6±1.2, 21.3±1.1, and 20.9±1.5, respectively), the saline-treated group showed a significantly higher GFAP staining index ($p<0.01$ for all) than the control group. Contrarily, the index was significantly lower in the PEG-treated group of rats (28.8±1.9, 25.1±0.8, and 27.9±0.8, respectively) as compared to the rats that received a placebo (table 2) (figures 3, 5). This was true for the CA1, CA3, and cerebellum.

The most characteristic byproduct of oxidative changes to DNA is 8-Oxo-dG, which has the potential to be the greatest non-invasive biomarker of DNA oxidative damage [50]. In our research, we used 8-Oxo -dG immunostaining to look into DNA oxidative damage in the CA1-CA3 areas of the hippocampus (Fig. 6). In keeping with the literature, saline-treated rats had significantly higher 8-Oxo-dG immunostaining indices (12.8±0.5 and 13.7±0.4, respectively) than non-irradiated rats (1.1±0.07 and 0.8±0.01, respectively). It is interesting to note that this index was statistically substantially lower ($p < 0.001$ for both) in PEG-treated rats (4.01±0.2 and 3.9±0.7, respectively) than in the rats in the placebo group (table 3) (figure 6).

The histopathological results obtained in our study reveal that PEG treatment significantly prevents or reduces apoptosis, astrogliosis, and oxidative DNA damage in rats.

Behavioral test

All results of behavioral tests are presented in table 3. Behavioral differences between rats in control, PEG-treated, and placebo groups were

[Downloaded from ijrr.com on 2026-11-09]

[DOI: 10.61186/ijrr.21.4.733]

evaluated in this part. We selected the PAL test since the hippocampus is one of the most commonly damaged brain regions by radiation, and thus cognitive problems including learning and memory are more likely [17, 36, 37]. There was a substantial difference (p<0.001) in the learning and memory performance of the placebo group rats (39.5±4.2 sec.) and the control group rats (265.1±22.3 sec.). In addition, rats in the PEG treatment group (181.5±30.4 sec.) showed a substantial improvement (p<0.001) in learning and memory ability compared to those in the placebo group (table 3).

Table 3. Comparative analysis of the effects of radiation therapy and PEG on behavioral test outcomes.

	Normal Control	Brain Irradiation + Saline	Brain Irradiation + PEG
Sociability test: The spend of time with stranger rat percentage (%)	59.5±1.7	25.2 ± 3.3 **	48.1 ± 2.9 ##
Open Field Test: Number of ambulation	12.5±0.8	4.1 ± 0.5 *	8.4 ± 0.8 #
Passive avoidance learning (PAL) Latency (Sec.)	265.1± 22.3	39.5 ± 4.2 **	181.5 ± 30.4 #

Results were presented as mean ± SEM. Statistical analyses were performed by one- way ANOVA. * p<0.01, ** p<0.001 different from normal groups; # p<0.05, ## p<0.001 different from Brain Irradiation and saline group.

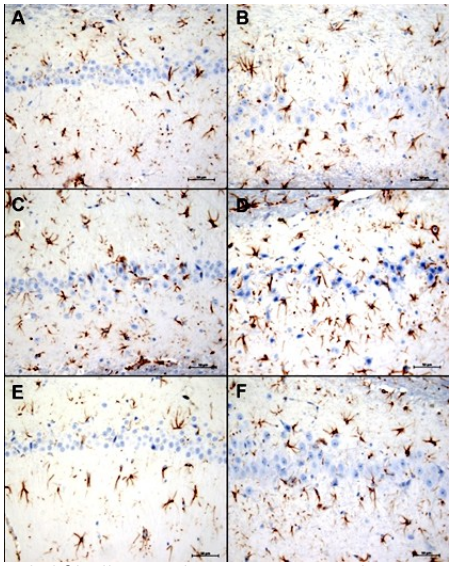


Figure 5. Glial fibrillary acidic protein -stained images of Cornu Ammonis 1 (CA1) **(A, C, E)** and CA3 regions **(B, D, F)** of the hippocampus with x40 magnification. **A-B:** In a rat in the control group, astrogliosis (brown staining) is observed within the normal range in the hippocampus regions. **C-D:** A saline-treated rat with whole brain irradiation (RAD) has a marked increase in gliotic activity in regions CA1 and CA3. **E-F:** In a rat treated with PEG 3350 in addition to RAD, gliotic activity was observed to be more limited than in the placebo group. (Scale bar= 50 µm).

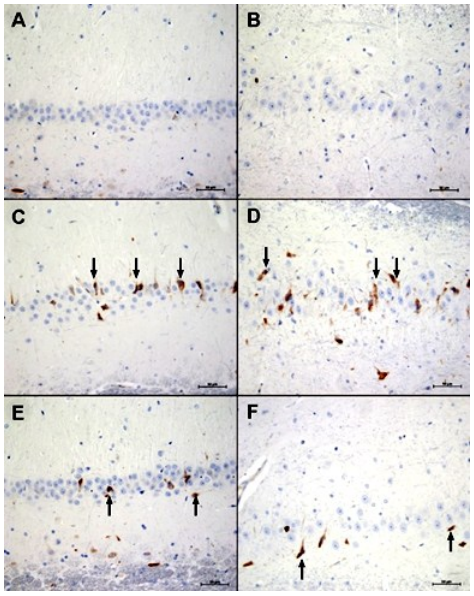


Figure 6. Images of the Cornu Ammonis 1 (CA1) **(A, C, E)** and CA3 regions **(B, D, F)** of the hippocampus at x40 magnification with 8-Oxo-2'-deoxyguanosine immunostaining used as a marker of oxidative damage to DNA. **A-B:** Normal appearance of hippocampus regions in a rat in the control group. **C-D:** A saline-treated rat with whole brain irradiation (RAD) shows changes in the CA1 and CA3 regions indicating oxidative damage to DNA. **E-F:** In a rat treated with PEG 3350 in addition to RAD, oxidative damage to DNA was observed to be more limited than in the placebo group. (Scale bar= 50 µm).

MR spectroscopy findings

On days 25 and 26, all rats were scanned using conventional MRI and MRS, and each rat was scanned for roughly 24 minutes. We concentrated on the lactate peak in the MRS imaging (figure 7) since it is related with an energy metabolism disruption caused by mitochondrial malfunction. Rats in the placebo group had higher (p<0.01) lactate peaks (367.6±20.5 % of control group) than rats in the control group, whereas the lactate peaks in MRS of rats treated with PEG (184.2±16.9 % of control group) were statistically closer (p<0.05) to those of rats in the control group than those of rats in placebo group (table 4).

Table 4. Comparative Analysis of the Effects of Radiation Therapy and PEG Based on MR Spectroscopy Results

	Normal Control	Brain Irradiation + Saline	Brain Irradiation + PEG
MR spectroscopy Lactate value (% of Normal Control)	100	367.6 ± 20.5 *	184.2 ± 16.9 #

Results were presented as mean ± SEM. Statistical analyses were performed by one- way ANOVA. * p < 0.001 different from normal groups; ## p < 0.001 different from Brain Irradiation and saline group.

[Downloaded from ijrr.com on 2026-11-09]

[DOI: 10.61186/ijrr.21.4.733]

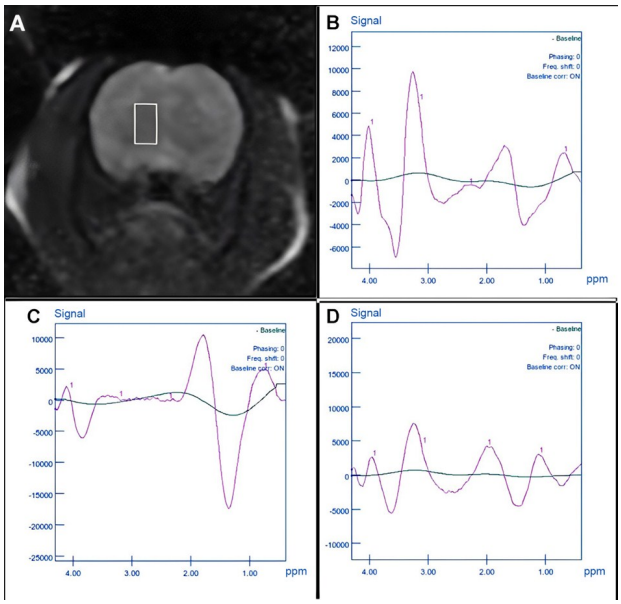


Figure 7. Magnetic resonance imaging (MRI) with spectroscopy. **A:** Coronal section T2-weighted image of the brain at the level of the right corpus striatum (white box) where spectroscopy measurements were made. **B:** MR spectrum showing metabolites in the brain of a rat in the control group. **C:** A marked increase in the amplitude of the lactate peak (1.3 ppm) is observed in the spectrum of a saline-treated rat with whole brain irradiation (RAD). **D:** In a rat treated with PEG 3350 in addition to RAD, the increase in lactate peak was more limited than in the placebo group.

DISCUSSION

In this study, biochemical analysis, histological results, and MR spectroscopy were used to show the neuroprotective benefits of PEG on rats with radiation-induced brain damage. This PEG therapeutic effect, which we measured using many metrics, was primarily caused by the stabilizing impact it had on membrane permeability. By lowering the production of free radicals, PEG-mediated plasma membrane repair indirectly reduces oxidative stress [49, 50]. Reactive oxygen species (ROSs) are produced by mitochondria during regular oxidative phosphorylation and released into the cytosol at higher rates after a number of pathological conditions where oxidative stress is a factor [51, 52]. As a result, mitochondria also play a significant role in oxidative stress. PEG may reduce oxidative stress in another way by interacting with and protecting the mitochondria, according to recent study [42, 53]. In a separate experiment, Juarez-Morino *et al.* found that the protective mechanism of PEG for peroxidases is based on the antioxidant property of PEG, which is able to remove or release radicals detrimental to the protein [54]. Since the main cause of radiation-related damage is the indirect oxidative effect of radiation on the production of ROS, which leads to the oxidation of macromolecules like DNA and lipids [13], it can be predicted that PEG can prevent radiation-related oxidation with its indirect antioxidant effects demonstrated by these three different mechanisms. The end outcome of lipid peroxidation is MDA, which is created when polyunsaturated fatty acids and free radicals interact. MDA may be utilized as a measure of cellular membrane degradation because lipids alter membrane characteristics by producing cross-linking between proteins and nucleic acids [55]. One of the primary byproducts of DNA oxidation is 8-Oxo-dG, and cell-level quantities of 8-Oxo-dG signal oxidative stress [56]. By using PEG, a potent membrane stabilizer, in our investigation, we were able to produce findings that were substantially closer to normal in terms of MDA levels and the 8-oxo-dG immunostaining index than we did with rats that did not get therapy (table 2 and figure 6). The fact that the brain tissue consumes around one-fifth of the body's oxygen [57] may provide some insight into the possible consequences of radiation-induced ROS damage. As a result, we believe that PEG's indirect antioxidant function is the primary mechanism behind its neuroprotective effects.

Microglia and astrocytes that detect neuronal injury surrounding them become activated as the first stage of an acute inflammatory response in the brain [58]. According to this theory, radiation causes inflammation by activating genes associated with it and boosting the synthesis of pro-inflammatory substances in brain tissue [59]. After exposure to radiation, NF-κB, various cell attachment components, and mediators like TNF-alpha, interleukin-1 beta (IL-1β), and interferon-gamma (IFN-γ) are all elevated [59, 60]. According to a number of studies, PEG may indirectly contribute to the activation of phagocytic microglia and a reduction in associated inflammatory responses by preventing necrosis [29, 30]. Impaired neurogenesis, particularly in the hippocampus, is partially caused by an increase in pro-inflammatory proteins, mainly NF-κB and TNF-α [61-63]. The hippocampus is crucial for memory, and it has been proposed that radiation-induced damage in hippocampal neurogenesis is connected to cognitive deficiencies in learning and memory [64, 65]. By administering PEG treatment to rats in our research, we were able to gain highly important information on neuroinflammation through NF-κB and TNF-α, neurogenesis by BDNF, and enhancement of memory skills via the PAL test (table 1 and 3).

Radiation-induced apoptotic cell death begins 3 to 4 hours after exposure and is one of the most important mechanisms in the early stages of RIBI [64, 66]. The hippocampus and cerebellum are among the brain regions where neuron and glial cell death are most common in apoptosis induced by a single dose of radiotherapy [67]. It has also been shown that the pro-inflammatory environment that develops secondary to damage to the irradiated brain regions

[Downloaded from ijrr.com on 2026-11-09]

[DOI: 10.61186/ijrr.21.4.733]

induces astrogliosis [31]. In addition to the resulting neuronal cell loss, astrocytes undergo proliferation, exhibit hypertrophic nuclei, and GFAP expression is increased [64]. In a study conducted by Baptiste D.C *et al*., it was noted that PEG has a protective effect that prevents damage to cytoskeleton proteins, resulting in reduced neuronal apoptosis [62]. Again, it is known that PEG is indirectly a non-immunogenic molecule with anti-inflammatory properties [43, 44]. In order to support these data, we found that there was a significant decrease in the number of cells and an increase in glial activity in the hippocampus and cerebellum after irradiation, while the pathological processes present in the rats in the PEG treatment group remained quite limited (figures 3-5). This protective effect of PEG on brain regions may be due to its ability to reach brain tissue as a result of radiation-induced endothelial cell death and permeability in the blood-brain barrier [31].

A shift in energy metabolism results in energy deprivation and eventual cell death because brain cells need ten times as much glucose and oxygen as other tissues [30]. The structure that is impacted in this process that results in cell death is the mitochondria, which are primarily in charge of generating cellular energy. Proper mitochondrial activity is crucial for preserving homeostasis, cellular integrity, and brain neurons because mitochondrial degeneration may result in cell body death owing to gradual axonal length reduction [68–71]. It is well known that radiation may directly harm mitochondria by triggering protein breakdown and resulting in cellular damage brought on by mitochondria, notably in the central nervous system [17]. Additionally, the mitochondrial permeability transition pore (MPTP), a protein found in the mitochondrial inner membrane that is typically closed, is stimulated to open by oxidative stress, which may be brought on by radiation, and this results in mitochondrial damage [72]. In addition to mending the injured plasma membrane, research by Chen *et al.* revealed that PEG has a neuroprotective impact by directly inhibiting MPTP [45]. Both biochemically and through MRS, we were able to demonstrate in our research that PEG has a protective impact on mitochondria, resulting in lower levels of cerebral lactate (tables 1, 4 and figure 7).

This study has several limitations that need to be taken into account. Firstly, we preferred to use PEG-3350 because its neuroprotective efficacy has been proven in several previous studies [73-75]. However, the concentration of PEG can change its effects; therefore, PEG polymers of different molecular weights can be used within a repeated dosing procedure to achieve the best results. Second, due to our focus on avoiding and minimizing acute radiation-induced brain injury, PEG's long-term effects on chronic radiation damage were not examined. Third, because we were interested in the effects of PEG on mitochondrial dysfunction, we did not use MR spectroscopy to explore metabolites other than lactate. Last, because we used an animal model to investigate the effects of PEG, we can't be certain that what we found holds true for humans.

CONCLUSION

In conclusion, this study suggests that Polyethylene glycol (PEG) could potentially mitigate radiation-induced brain injury (RIBI) in rats. PEG appears to offer neuroprotection largely through its beneficial impact on mitochondrial function, complemented by its antioxidant, anti-apoptotic, and anti-inflammatory properties secondary to membrane stabilization. Future investigations should aim to further validate PEG's molecular mechanisms of action using different molecular weights and dosage regimens.

***Declarations and ethical approval*:** The Animal Ethics Committee of Demiroglu Science University authorized the experimental procedures used in this study (Approval no: 4211121).

***Competing interests*:** The authors declare that they have no conflicts of interest.

***Authors' contributions*:** Conceptualization IHS, OE; Methodology IHS, BO, OA, NC; Software BO, MFB, MAE; Validation MFB, GY, OE; Formal analysis IHS, BO, MFB, NC; Investigation IHS, MAE, MFB, OE; Resources IHS, OA, GY; Data Curation BO, MFB, MAE, OE; Writing - Original Draft IHS, OA, MFB, OE; Writing - Review & Editing IHS, BO, GY, MAE, OE; Project administration IHS, OE.

***Funding*:** This research did not receive any specific grant from funding agencies in the public, commercial, or non-for-profit sectors.

***Availability of data and materials*:** The datasets generated during and/or analyzed during the current study are not publicly available but all are available from the corresponding author on reasonable request.

REFERENCES

1. Makale MT, McDonald CR, Hattangadi-Gluth JA, Kesari S (2017) Mechanisms of radiotherapy-associated cognitive disability in patients with brain tumours. *Nat Rev Neurol, **13**: 52-64*.
2. Johannesen TB, Lien HH, Hole KH, Lote K (2000) Radiological and clinical assessment of long-term brain tumour survivors after radiotherapy. *Radiother Oncol, **69**: 169-76*.
3. Brown PD, Pugh S, Laack NN, *et al.* Radiation Therapy Oncology Group (RTOG) (2013) Memantine for the prevention of cognitive dysfunction in patients receiving whole-brain radiotherapy: a randomized, double-blind, placebo-controlled trial. *Neuro Oncol, **15**: 1429-37*.
4. Cole AM, Scherwath A, Ernst G, *et al.* (2013) Self-reported cognitive outcomes in patients with brain metastases before and after radiation therapy. *Int J Radiat Oncol Biol Phys, **87**: 705-12*.
5. Beltran C, Naik M, Merchant TE (2010) Dosimetric effect of target expansion and setup uncertainty during radiation therapy in pediatric craniopharyngioma. *Radiother Oncol, **97**: 399-403*.

[Downloaded from ijrr.com on 2026-11-09]

[DOI: 10.61186/ijrr.21.4.733]

6. Béhin A and Delattre JY (2004) Complications of radiation therapy on the brain and spinal cord. *Semin Neurol,* ***24****: 405-17*.
7. Gorman AM, McGowan A, O'Neill C, Cotter T (1996) Oxidative stress and apoptosis in neurodegeneration. *J Neurol Sci,* ***139****: 45-52*.
8. Sezen O, Ertekin MV, Demircan B, *et al.* (2008) Vitamin E and L-carnitine, separately or in combination, in the prevention of radiation-induced brain and retinal damages. *Neurosurg Rev,* ***31****: 205-13*.
9. Steen RG, Spence D, Wu S, *et al.* (2001) Effect of therapeutic ionizing radiation on the human brain. *Ann Neurol,* ***50****: 787-95*.
10. Schnegg CI, Kooshki M, Hsu FC, *et al.* (2012) PPARδ prevents radiation-induced proinflammatory responses in microglia via transrepression of NF-κB and inhibition of the PKCα/MEK1/2/ ERK1/2/AP-1 pathway. *Free Radic Biol Med,* ***52****: 1734-43*.
11. Liu JL, Tian DS, Li ZW, *et al.* (2010) Tamoxifen alleviates irradiation -induced brain injury by attenuating microglial inflammatory response in vitro and *in-vivo*. *Brain Res,* ***1316****: 101-11*.
12. Zhao W and Robbins ME (2009) Inflammation and chronic oxidative stress in radiation-induced late normal tissue injury: therapeutic implications. *Curr Med Chem,* ***16****: 130-43*.
13. Kale A, Piskin Ö, Bas Y, *et al.* (2018) Neuroprotective effects of Quercetin on radiation-induced brain injury in rats. *J Radiat Res,* ***59****: 404-410*.
14. Hur W and Yoon SK (2017) Molecular Pathogenesis of Radiation-Induced Cell Toxicity in Stem Cells. *Int J Mol Sci,* ***18:*** *2749.*
15. Angelova PR and Abramov AY (2016) Functional role of mitochondrial reactive oxygen species in physiology. *Free Radic Biol Med,* ***100****: 81-85*.
16. Berezhnaya E, Neginskaya M, Uzdensky AB, Abramov AY (2018) Photo-ınduced oxidative stress ımpairs mitochondrial metabolism in neurons and astrocytes. *Mol Neurobiol,* ***55****: 90-95*.
17. Newton J, Brown T, Corley C, *et al.* (2020) Cranial irradiation impairs juvenile social memory and modulates hippocampal physiology. *Brain Res,* ***1748****: 147095*.
18. Casciati A, Dobos K, Antonelli F, *et al.* (2016) Age-related effects of X-ray irradiation on mouse hippocampus. *Oncotarget,* ***7****: 28040-58*.
19. Sharma NK, Stone S, Kumar VP, *et al.* (2019) Mitochondrial degeneration and autophagy associated with delayed effects of radiation in the mouse brain. *Front Aging Neurosci,* ***11****: 357*.
20. Koenig MK (2008) Presentation and diagnosis of mitochondrial disorders in children. *Pediatr Neurol,* ***38****: 305-13*.
21. Katsura M, Sato J, Akahane M, *et al.* (2021) Recognizing Radiation -induced Changes in the Central Nervous System: Where to Look and What to Look For. *Radiographics, 41: 224-248*.
22. Bonsi P, Cuomo D, Martella G, *et al.* (2006) Mitochondrial toxins in Basal Ganglia disorders: from animal models to therapeutic strategies. *Curr Neuropharmacol,* ***4****: 69-75*.
23. Lin MT and Beal MF (2006) Mitochondrial dysfunction and oxidative stress in neurodegenerative diseases. *Nature,* ***443****: 787-95*.
24. Tretter L, Sipos I, Adam-Vizi V (2004) Initiation of neuronal damage by complex I deficiency and oxidative stress in Parkinson's disease. *Neurochem Res,* ***29****: 569-77*.
25. Pfefferbaum A, Adalsteinsson E, Sullivan EV (2004*) In-vivo* structural imaging of the rat brain with a 3-T clinical human scanner. *J Magn Reson Imaging,* ***20****: 779-85*.
26. Yang YM, Feng X, Yao ZW, *et al.* (2008) Magnetic resonance angiography of carotid and cerebral arterial occlusion in rats using a clinical scanner. *J Neurosci Methods,* ***167****: 176-83*.
27. Aradi M, Steier R, Bukovics P, *et al.* (2011) Quantitative proton MRI and MRS of the rat brain with a 3T clinical MR scanner. *J Neuroradiol,* ***38****: 90-7*.
28. Dong X, Luo M, Huang G, *et al.* (2015) Relationship between irradiation-induced neuro-inflammatory environments and impaired cognitive function in the developing brain of mice. *Int J Radiat Biol,* ***91****: 224-39*.
29. Raju U, Gumin GJ, Tofilon PJ (2000) Radiation-induced transcription factor activation in the rat cerebral cortex. *Int J Radiat Biol,* ***76****: 1045-53*.
30. Hwang SY, Jung JS, Kim TH, *et al.* (2006) Ionizing radiation induces astrocyte gliosis through microglia activation. *Neurobiol Dis,* ***21****: 457-67*.
31. Yang L, Yang J, Li G, *et al.* (2017) Pathophysiological Responses in Rat and Mouse Models of Radiation-Induced Brain Injury. *Mol Neurobiol,* ***54****: 1022-1032*.
32. Zhou K, Boström M, Ek CJ, *et al.* (2017) Radiation induces progenitor cell death, microglia activation, and blood-brain barrier damage in the juvenile rat cerebellum. *Sci Rep,* ***7****: 46181*.
33. Sándor N, Walter FR, Bocsik A, *et al.* (2014) Low dose cranial irradiation-induced cerebrovascular damage is reversible in mice. *PLoS One,* ***9****(11): e112397*.
34. Ralcewicz TA and Persaud TV (1995) Effects of prenatal exposure to low dose ionizing radiation on the development of the cerebellar cortex in the rat. *Histol Histopathol,* ***10****: 371-83*.
35. Raber J, Rola R, LeFevour A, *et al.* (2004) Radiation-induced cognitive impairments are associated with changes in indicators of hippocampal neurogenesis. *Radiat Res,* ***162****: 39-47*.
36. Rola R, Raber J, Rizk A, *et al.* (2004) Radiation-induced impairment of hippocampal neurogenesis is associated with cognitive deficits in young mice. *Exp Neurol,* ***188****: 316-30*.
37. Georg Kuhn H and Blomgren K (2011) Developmental dysregulation of adult neurogenesis. *Eur J Neurosci,* ***33****: 1115-22*.
38. Turecek PL, Bossard MJ, Schoetens F, Ivens IA (2016) PEGylation of Biopharmaceuticals: A Review of chemistry and nonclinical safety ınformation of approved drugs. *J Pharm Sci,* ***105****: 460-475*.
39. Ivens IA, Achanzar W, Baumann A, *et al.* (2015) PEGylated Biopharmaceuticals: Current experience and considerations for nonclinical development. *Toxicol Pathol,* ***43****: 959-83*.
40. Pasut G, Panisello A, Folch-Puy E, *et al.* (2016) Polyethylene glycols: An effective strategy for limiting liver ischemia reperfusion injury. *World J Gastroenterol,* ***22****: 6501-8*.
41. Juarez-Moreno K, Ayala M, Vazquez-Duhalt R (2015) Antioxidant capacity of poly(Ethylene Glycol) (PEG) as protection mechanism against hydrogen peroxide ınactivation of peroxidases. *Appl Biochem Biotechnol,* ***177****: 1364-73*.
42. Luo J, Borgens R, Shi R (2002) Polyethylene glycol immediately repairs neuronal membranes and inhibits free radical production after acute spinal cord injury. *J Neurochem,* ***83****: 471-80*.
43. Ferrero-Andrés A, Panisello-Roselló A, Serafín A, *et al.* (2020) Polyethylene glycol 35 (PEG35) protects against ınflammation in experimental acute necrotizing pancreatitis and associated lung ınjury. *Int J Mol Sci,* ***21****: 917*.
44. Ackland GL, Gutierrez Del Arroyo A, Yao ST, *et al.* (2010) Low-molecular-weight polyethylene glycol improves survival in experimental sepsis. *Crit Care Med,* ***38****: 629-36*.
45. Chen H, Quick E, Leung G, *et al.* (2009) Polyethylene glycol protects injured neuronal mitochondria. *Pathobiology,* ***76****: 117-28*.
46. National Research Council (US) Committee for the Update of the Guide for the Care and Use of Laboratory Animals (2011) Guide for the Care and Use of Laboratory Animals. 8th ed. Washington (DC): National Academies Press (US).
47. Ji S, Tian Y, Lu Y, *et al.* (2014) Irradiation-induced hippocampal neurogenesis impairment is associated with epigenetic regulation of bdnf gene transcription. *Brain Res,* ***1577****: 77-88*.
48. Bradford MM (1976) A rapid and sensitive method for the quantitation of microgram quantities of protein utilizing the principle of protein-dye binding. *Anal Biochem,* ***72****: 248-54*.
49. Guo C, Li X, Wang R, *et al.* (2016) Association between oxidative DNA damage and risk of colorectal cancer: Sensitive determination of urinary 8-Hydroxy-2'-deoxyguanosine by UPLC-MS/MS Analysis. *Sci Rep,* ***6****: 32581*.
50. Gao Y, Wang P, Wang Z, *et al.* (2019) Serum 8-Hydroxy-2'-Deoxyguanosine Level as a Potential Biomarker of Oxidative DNA Damage Induced by Ionizing Radiation in Human Peripheral Blood. *Dose Response,* ***17****: 1559325818820649*.
51. Shi R and Borgens RB (2000) Anatomical repair of nerve membranes in crushed mammalian spinal cord with polyethylene glycol. *J Neurocytol,* ***29****: 633-43*.
52. Luo J, Borgens R, Shi R (2004) Polyethylene glycol improves function and reduces oxidative stress in synaptosomal preparations following spinal cord injury. *J Neurotrauma,* ***21****: 994-1007*.
53. Lenaz G, Bovina C, D'Aurelio M, *et al.* (2002) Role of mitochondria in oxidative stress and aging. *Ann N Y Acad Sci,* ***959****: 199-213*.
54. Halliwell B and Gutteridge JMC (1999) Free radicals in biology and medicine. *Oxford University Press, 1-897*.
55. Chen H and Shi R (2004) Polyethylene glycol improves function of isolated brain mitochondria: implication in central nervous system trauma. *J Neurotrauma,* ***21****: 1303*.
56. Halliwell B and Chirico S (1993) Lipid peroxidation: its mechanism, measurement, and significance. *Am J Clin Nutr,* ***57****: 715-724*.

[Downloaded from ijrr.com on 2026-11-09]

[DOI: 10.61186/ijrr.21.4.733]

57. de Souza-Pinto NC, Eide L, Hogue BA, *et al.* (2001) Repair of 8-oxodeoxyguanosine lesions in mitochondrial dna depends on the oxoguanine dna glycosylase (OGG1) gene and 8-oxoguanine accumulates in the mitochondrial dna of OGG1-defective mice. *Cancer Res, **61**: 5378-81*.
58. Valavanidis A, Vlachogianni T, Fiotakis K, Loridas S (2013) Pulmonary oxidative stress, inflammation and cancer: respirable particulate matter, fibrous dusts and ozone as major causes of lung carcinogenesis through reactive oxygen species mechanisms. *Int J Environ Res Public Health, **10**: 3886-907*.
59. Lipp LL (2014) Brain perfusion and oxygenation. *Crit Care Nurs Clin North Am, **26**: 389-98*.
60. Lumniczky K, Szatmári T, Sáfrány G (2017) Ionizing radiation-ınduced ımmune and ınflammatory reactions in the brain. *Front Immunol, **8**: 517*.
61. Fleming JC, Norenberg MD, Ramsay DA, *et al.* (2006) The cellular inflammatory response in human spinal cords after injury. *Brain, **129**: 3249-69*.
62. Baptiste DC, Austin JW, Zhao W, *et al.* (2009) Systemic polyethylene glycol promotes neurological recovery and tissue sparing in rats after cervical spinal cord injury. *J Neuropathol Exp Neurol, **68**: 661-76*.
63. Monje ML, Vogel H, Masek M, *et al.* (2007) Impaired human hippocampal neurogenesis after treatment for central nervous system malignancies. *Ann Neurol, **62**: 515-20*.
64. Balentova S and Adamkov M (2015) Molecular, cellular and functional effects of radiation-ınduced brain ınjury: A review. *Int J Mol Sci, **16**: 27796-815*.
65. Beamish CA, Zawaski JA, Inoue T, *et al.* (2021) NF-κB blockade by NEMO binding domain peptide ameliorates ınflammation and neurobehavioral sequelae after cranial radiation therapy in juvenile mice. *Int J Radiat Oncol Biol Phys, **109**: 1508-1520*.
66. Yang J, Gao J, Han D, *et al.* (2020) Hippocampal changes in inflammasomes, apoptosis, and MEMRI after radiation-induced brain injury in juvenile rats. *Radiat Oncol, **15**: 78*.
67. Tong F, Zhang J, Liu L, *et al.* (2016) Corilagin Attenuates Radiation-Induced Brain Injury in Mice. *Mol Neurobiol, **53**: 6982-6996*.
68. Greene-Schloesser D, Robbins ME, Peiffer AM, *et al.* (2012) Radiation-induced brain injury: A review. *Front Oncol, **2**: 73*.
69. Burchell VS, Gandhi S, Deas E, *et al.* (2010) Targeting mitochondrial dysfunction in neurodegenerative disease: Part I. *Expert Opin Ther Targets, **14**: 369-85*.
70. Saxton WM, Hollenbeck PJ (2012) The axonal transport of mitochondria. *J Cell Sci, **125**: 2095-104*.
71. Jing CH, Wang L, Liu PP, *et al.* (2012) Autophagy activation is associated with neuroprotection against apoptosis via a mitochondrial pathway in a rat model of subarachnoid hemorrhage. *Neuroscience, **213**: 144-53*.
72. Stansfield WE, Ranek M, Pendse A, *et al.* (2014) The pathophysiology of cardiac hypertrophy and heart failure. *Cell Mol Life Sci, **4**: 51-78*.
73. Brustovetsky N and Dubinsky JM (2000) Limitations of cyclosporin A inhibition of the permeability transition in CNS mitochondria. *J Neurosci, **20**: 8229-37*.
74. Zhang G, Rodemer W, Lee T, *et al.* (2018) The Effect of axon resealing on retrograde neuronal death after spinal cord ınjury in lamprey. *Brain Sci, **8**:65*.
75. Rodemer W and Selzer ME (2019) Role of axon resealing in retrograde neuronal death and regeneration after spinal cord injury. *Neural Regen Res, **14**: 399-404*.

[Downloaded from ijrr.com on 2026-11-09]

[DOI: 10.61186/ijrr.21.4.733]

[DOI: 10.61186/ijrr.21.4.733] [Downloaded from ijrr.com on 2026-11-09]